

We are IntechOpen, the world's leading publisher of Open Access books Built by scientists, for scientists

6,900

Open access books available

186,000

International authors and editors

200M

Downloads

Our authors are among the

154

Countries delivered to

TOP 1%

most cited scientists

12.2%

Contributors from top 500 universities



WEB OF SCIENCE™

Selection of our books indexed in the Book Citation Index
in Web of Science™ Core Collection (BKCI)

Interested in publishing with us?
Contact book.department@intechopen.com

Numbers displayed above are based on latest data collected.
For more information visit www.intechopen.com



The Ferroelectric-Ferromagnetic Composite Ceramics with High Permittivity and High Permeability in Hyper-Frequency

Yang Bai

*The University of Science and Technology Beijing
China*

1. Introduction

With the rapid development of portable electronic products and wireless technology, many electronic devices have evolved into collections of highly integrated systems for multiple functionality, faster operating speed, higher reliability, and reduced sizes. This demands the multifunctional integrated components, serving as both inductor and capacitor. As a result, low temperature co-fired ceramics (LTCC) with integrated capacitive ferroelectrics and inductive ferrites has been regarded as a feasible solution through complex circuit designs. However, in the multilayer LTCC structure consisting of ferroelectrics and ferrites layers, there are always many undesirable defects, such as cracks, pores and cambers, owing to the co-firing mismatch between different material layers, which will damage the property and reliability of end products (Hsu & Jean, 2005). A single material with both inductance and capacitance are desired for true integration in one element. For example, if the materials with both high permeability and permittivity are used in the anti electromagnetic interference (EMI) filters, the size of components can be dramatically minimized compared to that of conventional filters composed of discrete inductors and capacitors. Because little single-phase material in nature can meet such needs (Hill, 1999), the development of ferroelectric-ferromagnetic composite ceramics are greatly motivated.

Many material systems, such as BaTiO₃ / NiCuZn ferrite, BaTiO₃ / MgCuZn ferrite, Pb(Zr_{0.52}Ti_{0.48})O₃ / NiCuZn ferrite, Pb(Mg_{1/3}Nb_{2/3})O₃-Pb(Zn_{1/3}Nb_{2/3})O₃-PbTiO₃ / NiCuZn ferrite and Bi₂(Zn_{1/3}Nb_{2/3})₂O₇ / NiCuZn ferrite, were investigated and found exhibit fine dielectric and magnetic properties. In these reports, spinel ferrites, such as NiCuZn ferrite, were always used as the magnetic phase of composite ceramics, because they are mature materials for LTCC inductive components. However, the cut-off frequency of spinel ferrites is limited below 100MHz by the cubic crystal structure, so the resulting composite ceramics can not be used in hyper-frequency or higher frequency range. To keep up with the trend towards higher frequency for electronic technology, hexagonal ferrites, including Y-type hexagonal ferrite Ba₂Me₂Fe₁₂O₂₂ and Z-type hexagonal ferrite Ba₃Me₂Fe₂₄O₄₁ (Me=divalent transition metal), should be used in the composite ceramics.

Co₂Z hexagonal ferrite has high permeability and low loss in hyper-frequency, but the very high sintering temperature (>1300°C) works against its application in LTCC. Y-type hexagonal ferrite has a bit lower permeability, but the excellent sintering behavior makes it a

good candidate of magnetic material in LTCC. To achieve high dielectric permittivity, lead-based relaxor ferroelectric ceramics is a good choice as the ferroelectric phase in the composite ceramics owing to its high dielectric permittivity and low sintering temperature. In this chapter, we summarize the co-firing behavior, microstructure and electromagnetic properties of the composite ceramics for hyper-frequency. The material system is mainly focused on a composite ceramics composed of $0.8\text{Pb}(\text{Ni}_{1/3}\text{Nb}_{2/3})\text{O}_3$ - 0.2PbTiO_3 (PNNT) and $\text{Ba}_2\text{Zn}_{1.2}\text{Cu}_{0.8}\text{Fe}_{12}\text{O}_{22}$ (BZCF), which has excellent co-firing behavior and good electromagnetic properties in hyper-frequency, and some other composite ceramics are also involved in some sections.

2. The co-firing behavior, phase composition and microstructure

2.1 The co-firing behavior and densification

Due to the different sintering temperatures and shrinkage rates of ferroelectric phase and ferromagnetic phase, remarkable co-firing mismatch often occurs and results in undesirable defects, such as cracks and cambers. As a result, the property of composite ceramics and the reliability of end products are damaged. Thanks to the existence of large amount of grain boundaries to dissipate stress, the composite ceramics with powder mixture have much better co-firing behavior than the multilayered composite ceramics. Although the mismatch of densification rate is alleviated to a larger extent, a good sintering compatibility between ferroelectric and ferromagnetic grains is still required for better co-firing match. The starting temperature of shrinkage and the point of maximum shrinkage rate are both important for the co-firing behavior of composite ceramics. Some research indicates that the composite ceramics exhibits an average sintering behavior between two phases and the shrinkage rate curve of composite ceramics is between those of two component phases (Qi et al., 2008).

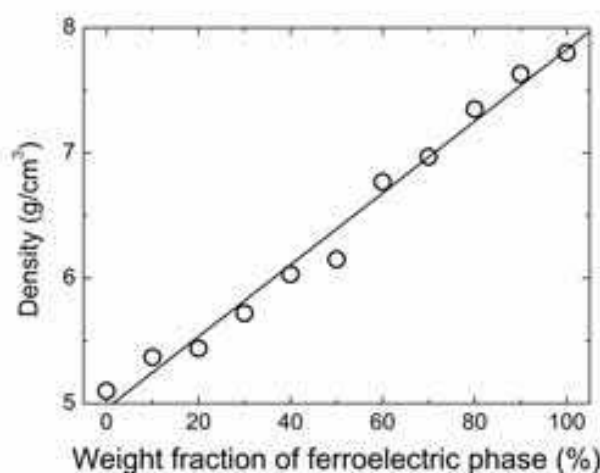


Fig. 1. The density of the sintered PNNT-BZCF composite ceramics as a function of the weight fraction of ferroelectric phase

Y-type hexagonal ferrite has a lower sintering temperature of $1000\sim 1100^\circ\text{C}$, which is similar to that of lead-based ferroelectric ceramics. For example, in PNNT-BZCF composite material, BZCF has a sintering temperature of 1050°C , same as that of PNNT. Hence, the composite system has good co-firing behavior for each composition (Bai et al., 2007). After sintered at 1050°C , all the samples exhibit a high density, above 95% of theoretical density. Fig. 1 shows the composition dependence of the density of sintered PNNT-BZCF composite

ceramics. Since the density of a composite material is the weighted average of those of constituent phases, it increases linearly with the rise of weight fraction of ferroelectric phase. Similar relationship is obtained in other composite materials (Qi et al., 2004 & Shen et al., 2005).

2.2 The element diffusion

The element diffusion always occurs between two phases during the sintering process at high temperature. The thickness of diffusion layer and element distribution influence microstructure and properties of composite ceramics. The diffusion coefficient is determined by the ion's radius and charge. Table 1 shows the radius of some ions commonly used in ferroelectric ceramics and ferrite.

Ba ²⁺	Pb ²⁺	Ti ⁴⁺	Nb ⁵⁺	Fe ³⁺	Fe ²⁺	Co ²⁺	Zn ²⁺	Cu ²⁺	Mn ³⁺	Ni ²⁺
0.135	0.120	0.068	0.07	0.076	0.064	0.074	0.074	0.072	0.066	0.072

Table 1. The radius of some ions

It is always thought that Ba²⁺ ion does not diffuse due to the large radius, which has been confirmed by experiments. Although Pb²⁺ also has large radius, the low vapor pressure make it to easily escape from lattice at high temperature. The deficiency of Pb²⁺ in the lattice can result in the formation of pyrochlore phase. For the metallic ion in ferrite, the diffusion coefficient can be ranked as $D_{Co} > D_{Fe} > D_{Zn} > D_{Ni}, D_{Cu}$ based on the experiments of atomic emission spectrometry (AES) and electron probe micro-analyzer (EPMA). Fig. 2 (a) and (b) show the backscattered electron image and element distribution around the interface in the composite ceramics consisting of Pb(Mg_{1/3}Nb_{2/3})O₃ and NiCuZn ferrite. The diffusion of different ions between ferroelectric grain and ferromagnetic grain is clear.

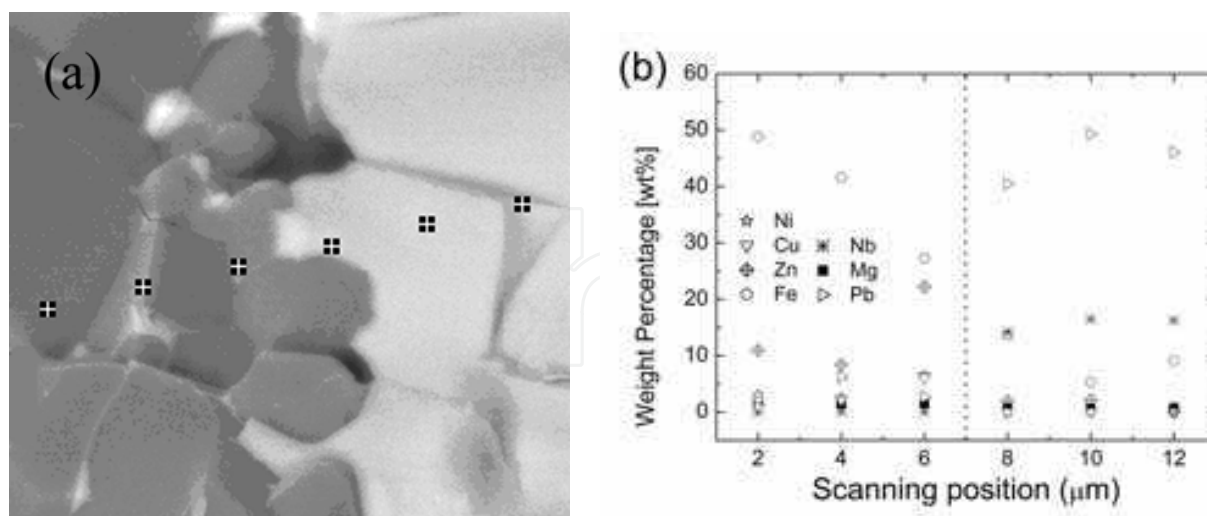


Fig. 2. (a) the backscattered electron image and (b) element distribution around the interface of the composite ceramics of Pb(Mg_{1/3}Nb_{2/3})O₃-NiCuZn ferrite

The element diffusion can influence the microstructure and electromagnetic properties of composite ceramics. For example, the grains at the interface of two phases may grow abnormally large. To alleviate the element diffusion, lowering the sintering temperature is a feasible solution.

2.3 Phase composition crystal structure

During the co-firing process, chemical reactions may take place at the interface of two phases and produce some new phases, which affect the properties of co-fired composite ceramics. For example, pyrochlore phase is often formed in the composite ceramics with lead-based ferroelectric ceramics due to Pb volatilization. Fig. 3 shows a X-ray diffraction (XRD) spectrum of the composite ceramics of 40wt% $\text{PbMg}_{1/3}\text{Nb}_{2/3}\text{O}_3$ -60wt%NiCuZn ferrite, which clearly shows the existence of pyrochlore phase. If the sintering temperature is lowered below 1000°C, the volatilization of Pb can be largely reduced, so does the formation of pyrochlore phase.

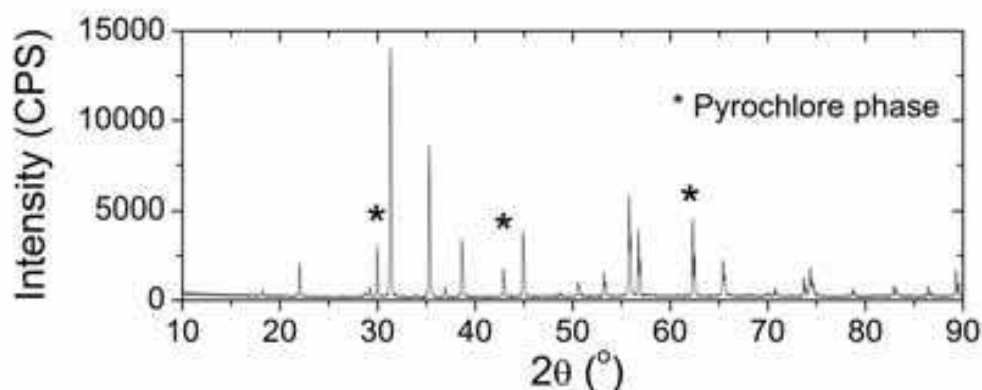


Fig. 3. XRD spectrum of the composite ceramics of 40wt% $\text{PbMg}_{1/3}\text{Nb}_{2/3}\text{O}_3$ -60wt%NiCuZn ferrite

Fig. 4 compares the XRD spectra of PNNT-BZCF composite ceramics before and after sintering process. According to the XRD spectra, no other phase is found after co-firing process, i.e. no obvious chemical reaction takes place between PNNT and BZCF during the sintering process of 1050°C.

It is clear that only perovskite phase can be detected in the XRD spectra of samples either before or after co-firing process, if the weight fraction of PNNT is higher than or equals to 0.8. It is because that the crystal structure of Y-type hexagonal ferrite is more complex than the perovskite structure of ferroelectric phase, which results in a much lower electron density. In addition, for the sample with same volume fraction of PNNT and BZCF, the XRD intensity of perovskite phase is much stronger than that of BZCF due to the same reason. With the rise of BZCF amount, the intensities of its diffraction peaks gradually enhance. Up to the weight fraction of ferroelectric phase is as low as $x=0.1$, the XRD peaks of perovskite phase are still obvious in the XRD spectrum.

The crystal morphology and orientation may be changed due to the different densification characters of two phases in the co-firing process (Bai et al., 2009). It is noticed from Fig. 4 that the relative intensity of the diffraction peaks of Y-type hexagonal ferrite changes after the co-firing process. For the green samples, the primary diffraction peak of BZCF is at 30.4° corresponding to (110) plane, which is same as the pure Y-type hexagonal ferrite; while the primary peak is at 32° corresponding to (10 $\bar{1}$ 3) plane for the sintered samples, which is the secondary peak of pure Y-type hexagonal ferrite. This variation of XRD intensities of Y-type hexagonal ferrite after co-firing process is well indexed by comparing the sintered samples of $x=0$ and $x=0.1$ in Fig. 5. The change reflects a lattice distortion induced by the internal stress.

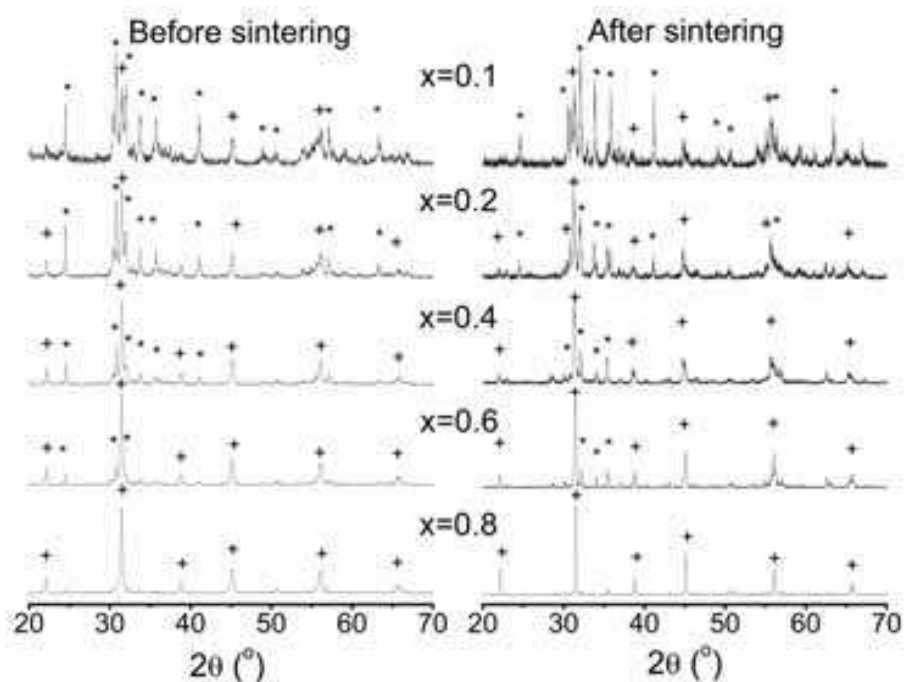


Fig. 4. XRD spectra of PNNT-BZCF composite ceramics before and after sintering at 1050°C (+ : perovskite phase, PNNT; * : Y-type hexagonal ferrite, BZCF).

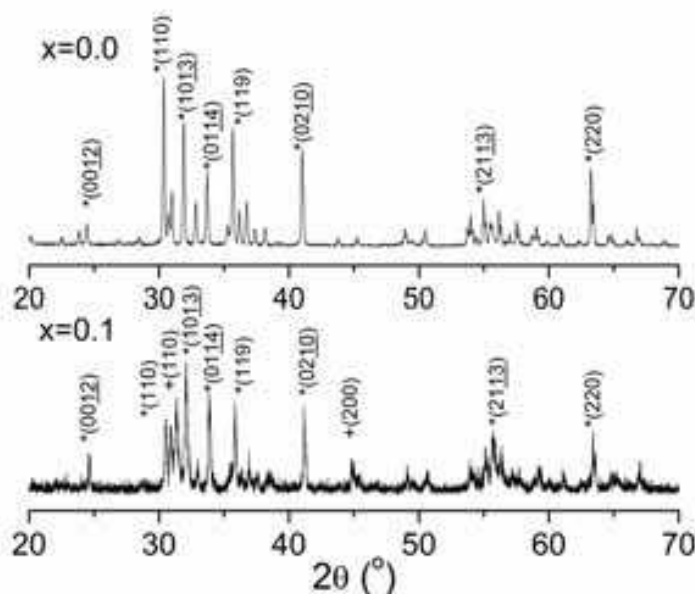


Fig. 5. XRD spectra comparison of 10wt%PNNT-90wt%BZCF composite ceramics and pure Y-type hexagonal ferrite (+ : perovskite phase, PNNT; * : Y-type hexagonal ferrite, BZCF)

2.4 Microstructure

When the sintering temperatures of two constituent phases are greatly different, the co-firing mismatch will result in various defects in the microstructure of co-fired composite ceramics. If two phases have similar sintering temperature, the co-firing mismatch will be slight.

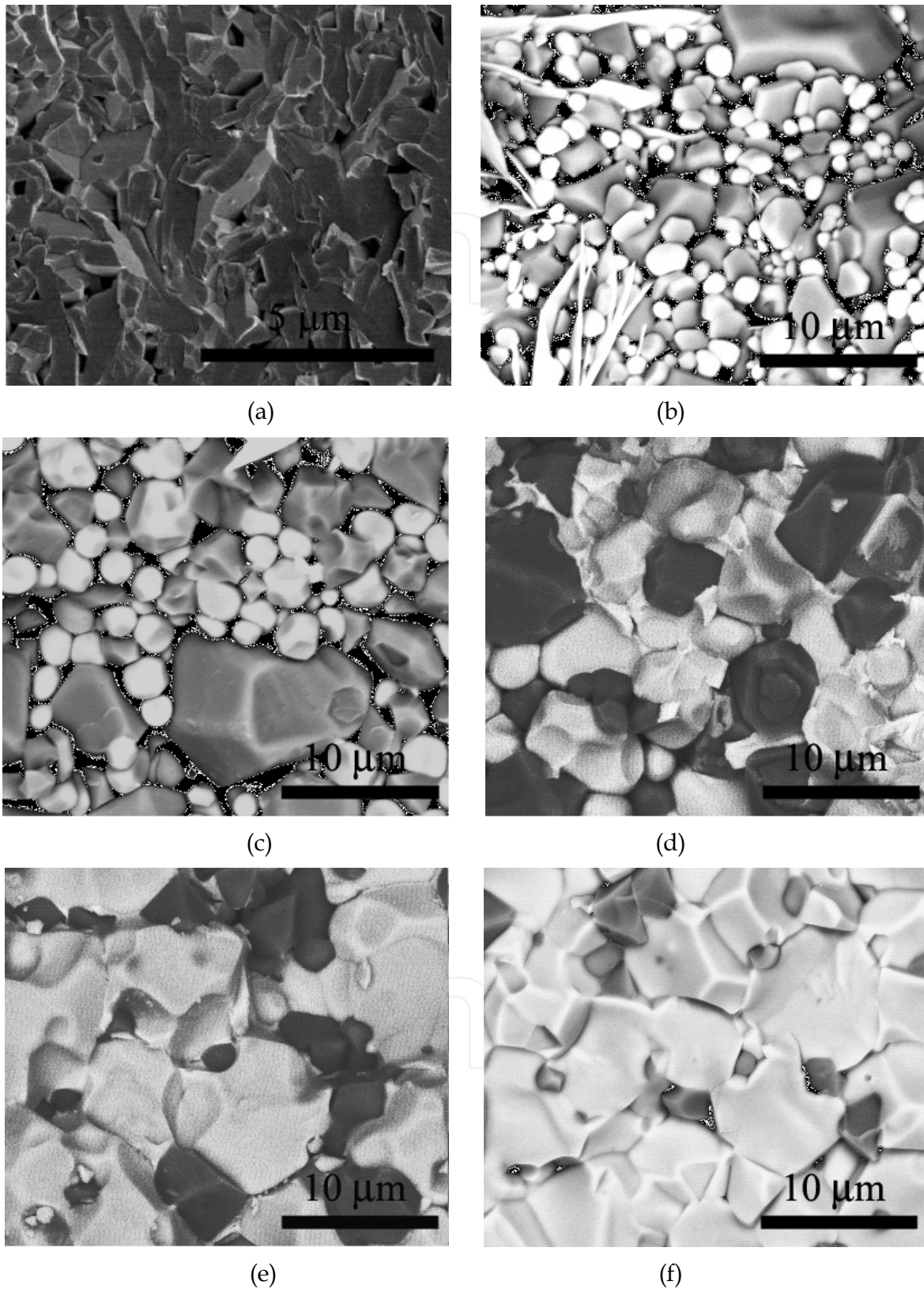


Fig. 6. The microstructure of PNNT-BZCF composite ceramics (a) $x=0$ (b) $x=0.2$ (c) $x=0.3$ (d) $x=0.5$ (e) $x=0.7$ (f) $x=0.9$ [(a) is secondary electron image, while (b)-(f) are backscattered electron images.]

Fig. 6 (a)-(f) show the scanning electron microscope (SEM) images of the microstructure of PNNT-BZCF composite ceramics. In backscattered electron image, the grains of PNNT and BZCF respectively appear white and gray due to the difference of molecular weights of the elements in them. The sintered samples exhibit dense microstructures for each composition and the grains of PNNT and BZCF distribute homogeneously. It indicates that this composite system has a fine co-firing behavior over a wide composition range, which thanks to the same sintering temperature of PNNT and BZCF.

The average size of ferroelectric or ferrite grains decreases with the rise of corresponding phase amount. For example, as BZCF content is low, few ferrite grains are besieged by large amount of PNNT grains. It becomes difficult for small ferrite grains to merge with the neighboring likes. With the increase of ferrite's content, the chance of amalgamation of small grains rises, and then grains grow larger. The thing is same for PNNT grains.

From the SEM images, it is noticed that the grain morphology of ferrite changes obviously with composition. In the sample of pure Y-type hexagonal ferrite ($x=0$), the grains are platelike and many of them are of hexagonal shape [Fig. 6 (a)]. In the co-fired ceramics [Fig. 6(b)-(f)], the planar grains of hexagonal ferrite become equiaxed crystals just as those ferroelectric grains. During the co-firing process, the grain growth of two constituent phases is affected each other. Because equiaxed crystal is more favorable for a compact-stack microstructure than planar crystal, the surrounding equiaxed grains of PNNT modulate the grain growth of BZCF particles and assimilate their grain shape into equiaxed crystal during the co-firing process. It is well known that the internal stress is unavoidable in the co-fired ceramics. In BZCF-PNNT composite ceramics, the compact-stacked grains and the change of BZCF's grain morphology suggest the existence of internal stress and lattice distortion, which are also reflected in XRD spectra as discussed in prior section.

3. The static electromagnetic properties

3.1 The ferroelectric hysteresis loop

For the ferroelectric-ferromagnetic composite ceramics, the ferroelectric or ferromagnetic character is determined by the corresponding phase, while the magnetoelectric effect is always weak. To examine the ferroelectricity of composite ceramics, the ferroelectric polarization-electric field (P-E) hysteresis loop is the most important character.

For PNNT-BZCF composite ceramics, the P-E hysteresis loops are observed over the whole composition range (Fig. 7), which implies the ferroelectric nature of composite ceramics. The maximum polarization P_{\max} decreases with the reduction of ferroelectric phase due to dilution effect, which indicates that the ferroelectricity of composite ceramics originates from the nature of ferroelectric phase.

It is also noted that the shape of P-E loop varies with composition. The sample with high PNNT amount ($x>0.8$) has fine and slim hysteresis loop, while the sample with relative less ferroelectric phase has an open-mouth-shaped P-E loop. It is because that the ferrite has much lower electric resistivity of about $10^6 \Omega \text{ cm}$ than that of ferroelectric ceramics (above $10^{11} \Omega \text{ cm}$). In the ferroelectric-ferromagnetic composite ceramics, the ferrite grains serve as a conductive phase in the electric measurement, especially under a high electric field. If the ferrite content is low, the small ferrite grains are besieged by the ferroelectric grains with high resistivity and there is no conductive route in the microstructure. As a result, the composite ceramics has high resistivity and low leak current. With the rise of ferrite amount, the percolation occurs in the composite system and the resistivity drops remarkably (Qi et al., 2004 & Bai et al., 2007). The large leak current results in an open-mouth-shaped P-E loop.

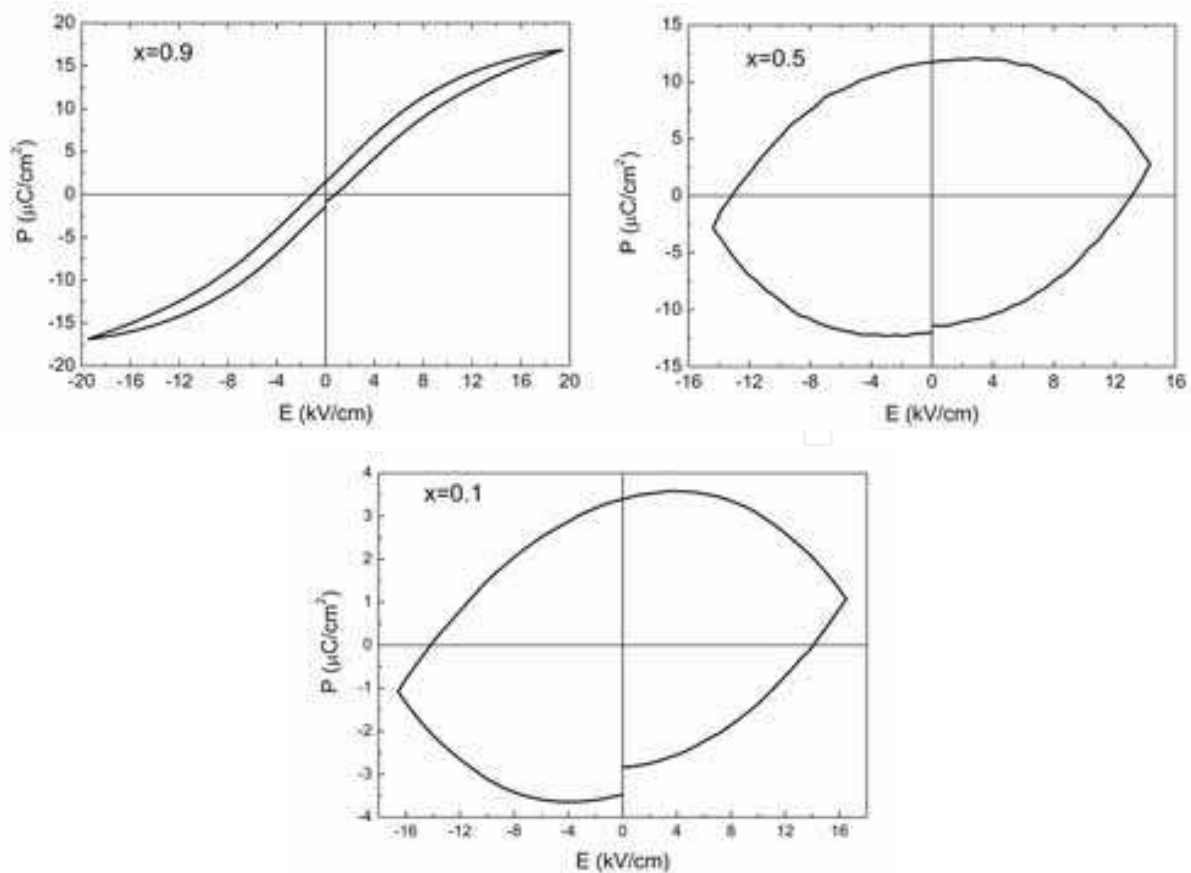


Fig. 7. P-E hysteresis loops of PNNT-BZCF composite ceramics (a) $x=0.9$; (b) $x=0.5$; (c) $x=0.1$

3.2 The ferromagnetic hysteresis loop

The magnetic hysteresis loop is the best experimental proof for the ferromagnetic nature of materials. Up to now, none of ferroelectric ceramics exhibits ferromagnetic character at room temperature, so the ferromagnetic behaviors of composite ceramics are dominated by the ferrite phase. For the application in high frequency, soft magnetic material is needed for the composite materials.

The magnetic hysteresis loops of PNNT-BZCF composite ceramics is plotted in Fig. 8. The ferromagnetic characters of composite ceramics are only inherited from those of the magnetic phase of Y-type hexagonal ferrite, so all the samples exhibit soft magnetic character with low coercive force H_c and low remnant magnetization M_r . The coexistence of magnetic hysteresis loop and P-E loop implies that the PNNT-BZCF composite ceramics have both ferromagnetic and ferroelectric properties at room temperature, which also confirms the possibility to achieve both high permittivity and permeability.

Fig. 9 shows the composition dependence of M_s , M_r and H_c for PNNT-BZCF composite ceramics before and after sintering process. For the green sample before sintering, M_s and M_r both decrease monotonously with the reduction of BZCF amount, while H_c keeps a constant. The magnetic properties of green samples are dominated by the nature of individual magnetic particles and there is little interaction between constituent phases due to loose microstructure. The linear decrease of M_s and M_r is only a result of dilution effect. The small ferrite particles and lots of defects in microstructure endow the green samples a relatively high H_c , which is insensitive to the variation of composition.

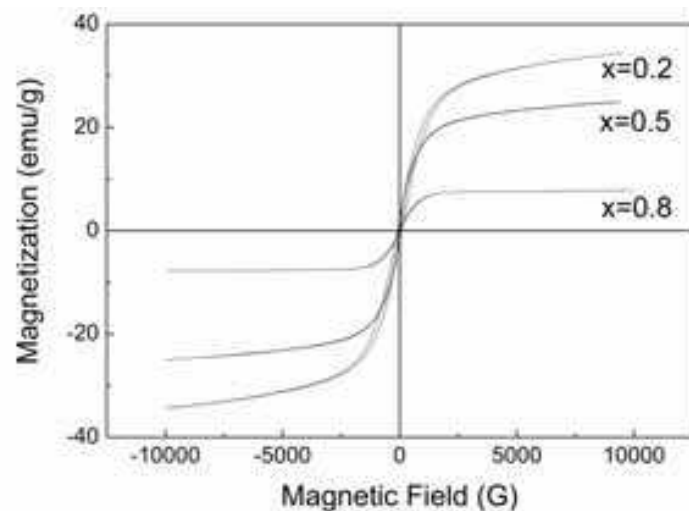


Fig. 8. The magnetic hysteresis loops of PNNT-BZCF composite ceramics

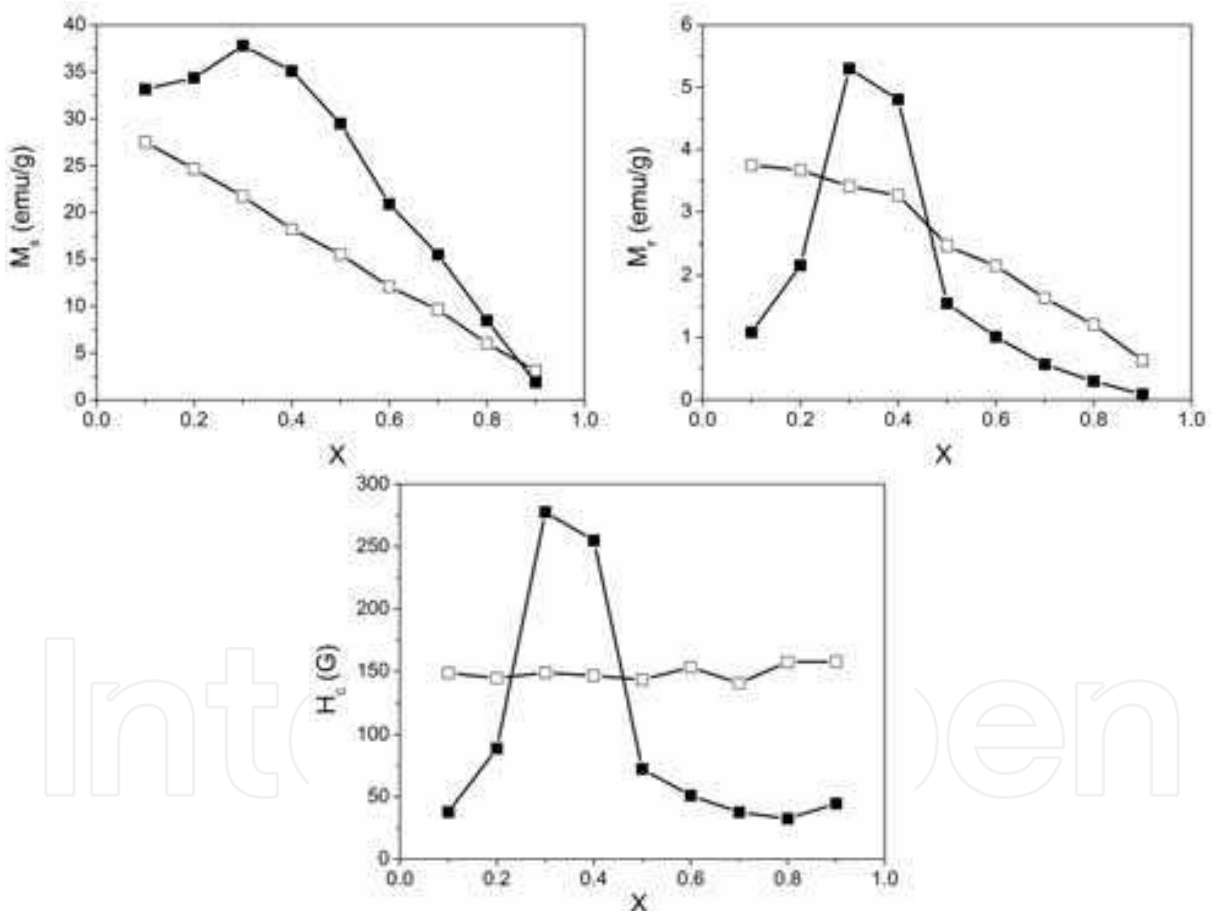


Fig. 9. The composition dependence of (a) M_s , (b) M_r and (c) H_c for the composite ceramics of PNNT-BZCF before (□) and after (■) sintering process

After the sintering process, M_s decreases monotonously with the reduction of ferrite amount if the mechanical interaction between two constituent phases is weak. For example, M_s varies near linearly with the ferrite content in $BaTiO_3$ -NiCuZn ferrite or PMNZT-NiCuZn ferrite composite ceramics, where ferroelectric phase and ferrite phases are both of equiaxial grains and little internal stress is produced after co-firing process (Qi et al., 2004).

If the microstructure varies notable after co-firing process, the magnetic properties of composite ceramics will be affected (Bai et al., 2009). With the reduction of BZCF amount in PNNT-BZCF composite materials, M_s , M_r and H_c of the sintered samples increase first, reach a maximum at $x=0.3$, and then decrease (Fig. 9). The enhancement of M_s in the range of $0.1 < x < 0.3$ originates from the internal stress produced in the co-firing process. It is reported that the structural distortion can generate spontaneous magnetization in several composite materials (Kanai et al., 2001 & Kumar et al., 1998). In PNNT-BZCF composite ceramics, the enhancement of M_s in the range of $0.1 < x < 0.3$ is also thought as a result of the internal stress induced structural distortion, which has been detected by XRD spectra and SEM images. A more notable enhancement of M_r and H_c is observed in the range of $0.1 < x < 0.3$, because M_r and H_c are more sensitive to the microstructure. The stress on ferrite grains increases the resistance of domain wall's motion and spin rotation, so the magnetization reversal under external magnetic field becomes more difficult, which is reflected as the increase of M_r and H_c . When ferrite's amount decreases further, the dilution effect dominates the magnetic properties of composite ceramics, and then M_s , M_r and H_c decline monotonically.

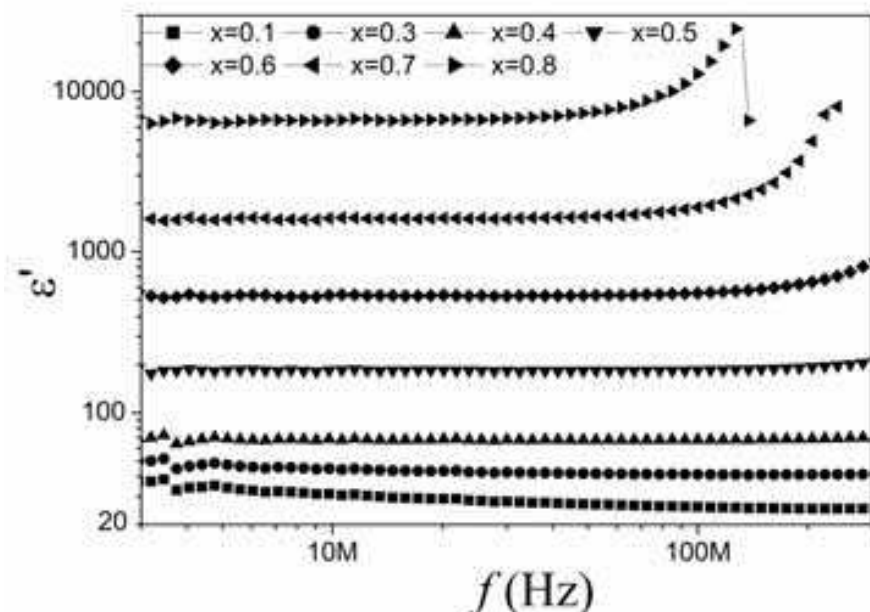


Fig. 10. Frequency dependence of permittivity of PNNT-BZCF composite ceramics

4. The permittivity and permeability in hyper-frequency

4.1 Permittivity

Owing to the polarization of dipolar, ferroelectric ceramics always have significant permittivity higher than several thousands, while the permittivity of ferrite may be as low as ~ 20 . The dielectric mechanism of ferrite is associated with the conduction mechanism, which is attributed to the easy electron transfer between Fe^{2+} and Fe^{3+} . Although some ferrite containing large amount of Fe^{2+} ions has high permittivity of several thousands, such as MnZn ferrite, the low electric resistivity limits its application in high frequency. When the sintering temperature is lower than $1100^{\circ}C$ or the sample is sintered under high partial pressure of oxygen, the sample has high resistivity and low permittivity of ~ 20 , which is suitable for the application in high frequency.

The permittivity of two-phased composite material is always between those of two constituent phases and controlled by their relative volume fractions. Since the permittivity of ferroelectric ceramics is much higher than that of ferrite, the composite ceramics with more ferroelectric phase have higher permittivity. Fig. 10 shows the frequency dispersion of permittivity of PNNT-BZCF composite ceramics. The permittivity increases monotonically with the rise of PNNT amount. For example, the permittivity increases from 30 to 6600 (@ 10MHz) when the weight fraction of PNNT rises from 0.1 to 0.8.

4.2 Permeability

The permeability of nonmagnetic ferroelectric ceramics is always one, while the soft magnetic ferrites have high permeability. Due to the inverse proportion of permeability and cut-off frequency, the permeability turns lower in higher frequency range, which is associated with the magnetic structure of material. For example, the permeability of NiZn and MnZn spinel ferrites is higher than several thousands below MHz frequency range, but it turns very low above MHz, that is attributed to their cubic structure. The hexagonal ferrites, especially Y-type hexagonal ferrite, have planar magnetocrystalline anisotropy, which endows them high permeability above 100MHz. Because the ferrite has much higher permeability than ferroelectric ceramics, the permeability of composite ceramics increases with the rise of ferrite's amount (Fig. 11).

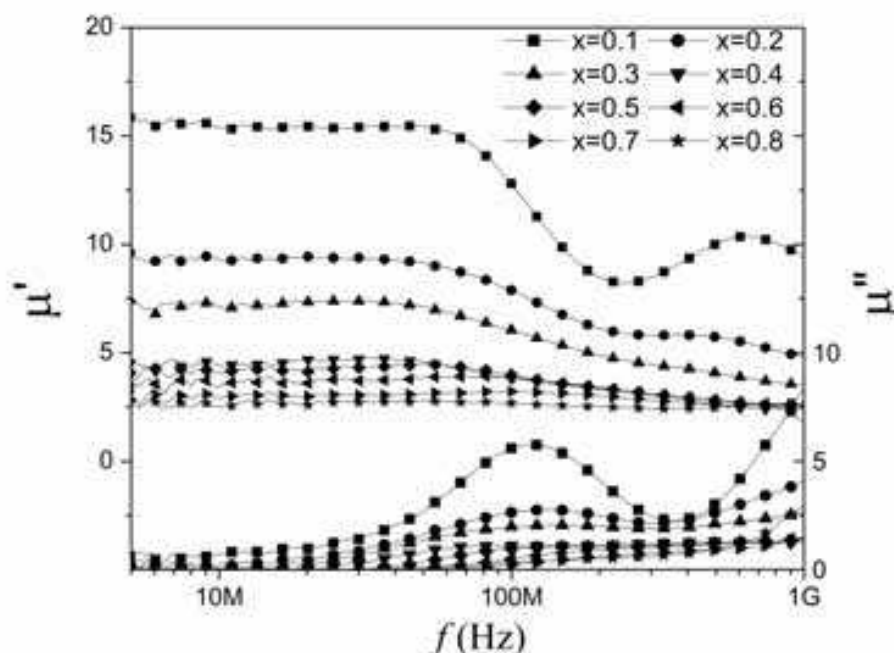


Fig. 11. Frequency dependence of real part and imaginary part of complex permeability of the composite ceramics of PNNT-BZCF ($x=0.1\sim 0.8$)

4.3 The theoretical prediction

The effective macroscopic electromagnetic properties of a composite material are determined by the intrinsic characters of constituent phases and their relative volume fractions, so some mixture theories and equations have been established based on an equivalent dipole representation to predict the electromagnetic properties of a composite

material. In this section, three most popular mixture theories are introduced, including mixture law, Maxwell-Garnett equations (containing MGa, MGb) and Bruggeman effective medium theory (EMT).

The mixture law is the simplest mixture theory to predict the properties of a composite material. According to the structure type of a composite material, the mixture law has different forms, such as parallel connection model and series connection model. For the composite material with powder mixture, the mixture law has a form as

$$\ln \Psi^* = f_a \ln \Psi_a + f_b \ln \Psi_b \quad (1)$$

where Ψ^* , Ψ_a and Ψ_b are the effective dielectric permittivity or magnetic permeability of composite material and two constituent phases. The f_a and f_b refer to the volume fraction of two phases and $f_a + f_b = 1$.

Further, some mixture theories are developed based on an equivalent dipole representation of the mixture, where the effective macroscopic electromagnetic properties of composite material are modeled as the intrinsic dipole moments per unit volume of each constituent phase and the relative volume fraction. It is assumed that the isolated particles of constituent phases are embedded in a matrix host. The electric and magnetic intrinsic dipole moments of component phases, as well as those of matrix host, are used to calculate the effective macroscopic properties of composite material. In static (or quasistatic) regime, a general form of the mixture equation was established based on the assumption that the components of isolated particles are embedded in a contiguous host medium (Aspnes, 1982). It can be expressed as

$$\frac{\Psi^* - \Psi_h}{\Psi^* + 2\Psi_h} = f_a \frac{\Psi_a - \Psi_h}{\Psi_a + 2\Psi_h} + f_b \frac{\Psi_b - \Psi_h}{\Psi_b + 2\Psi_h} \quad (2)$$

where Ψ_h is the effective permittivity or permeability of the host medium. If the host material is chosen as either phase **a** or **b**, Maxwell-Garnett mixture equations, including MGa and MGb equations, are obtained (Maxwell Garnett, 1904 & 1906). If phase **a** is chosen as the host material, Equation (2) can be simplified to MGa equation as

$$\frac{\Psi^* - \Psi_a}{\Psi^* + 2\Psi_a} = f_b \frac{\Psi_b - \Psi_a}{\Psi_b + 2\Psi_a} \quad (3)$$

Similarly, MGb equation is derived as

$$\frac{\Psi^* - \Psi_b}{\Psi^* + 2\Psi_b} = f_a \frac{\Psi_a - \Psi_b}{\Psi_a + 2\Psi_b} \quad (4)$$

Different values of Ψ^* can be calculated using MGa and MGb equations for a composite material with a given volume fraction of particles. It is because the properties of matrix host are dominated until the volume fraction of isolated particle closely approaches unity. This expression works fairly well provided the inclusions make up a small fraction of the total volume. However, the Maxwell-Garnett model omits the variation of microstructure, so the imbedded phase never percolates even when the matrix has obviously inverted.

To characterize the microstructural inversion, Bruggeman effective medium theory is formed (Bruggeman, 1935), where the host material is chosen as the mixture itself ($\Psi^* = \Psi_h$), and then Equation (2) is reduced as

$$0 = f_a \frac{\Psi_a - \Psi_h}{\Psi_a + 2\Psi_h} + f_b \frac{\Psi_b - \Psi_h}{\Psi_b + 2\Psi_h} \quad (5)$$

Bruggeman effective medium theory assumes that component **a** and **b** are both embedded in the effective medium itself and are not treated as contiguous constituents, so it can predict percolation of either phase when its volume fraction is over 1/3. Its predictions exhibit a significant improvement compared with MG equations. This formalism has more applicability for composites formed by the constituents with similar mechanical properties. In this section, component **a** and **b** are chosen as ferroelectric ceramics and ferrite, respectively. To exclude the influence of frequency dispersion, the experimental data of permittivity or permeability are accessed in region where the value is steady within a wide frequency range.

Fig. 12 compared the measured permittivity and calculated values by different equations for PNNT-BZCF composite ceramics. Mixture law and MGa equation give good predictions of permittivity for the composite ceramics with less ferroelectric phase, while the calculated results greatly deviates from the experimental data if PNNT's amount is large. On the contrary, MGb equation works well only if PNNT's amount is very high. EMT result matches the experimental data well if one phase has much higher volume fraction than the other, but it does not work well when two phases have comparable volume fraction. In addition, MGa and MGb equations offer upper and lower limits for the permittivity of PNNT-BZCF composite ceramics.

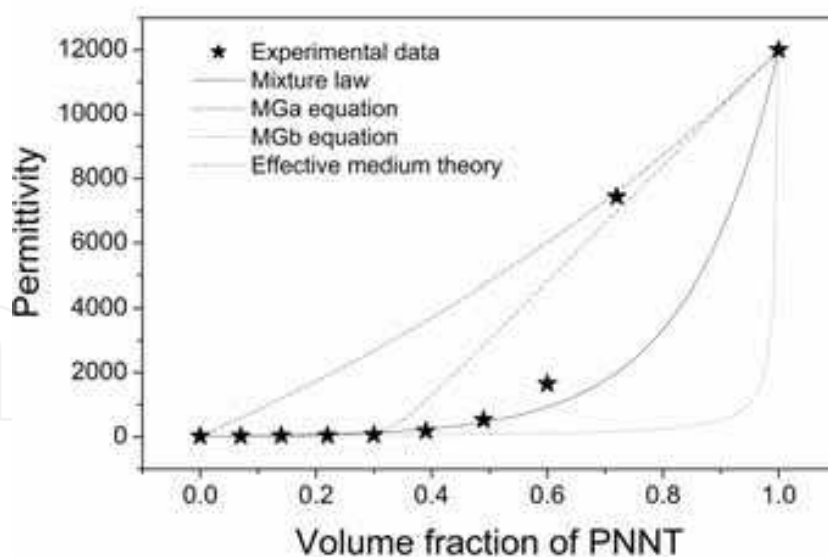


Fig. 12. The composition dependence of measured and calculated permittivity of PNNT-BZCF composite ceramics

The theoretical predicted permeability and experimental data of PNNT-BZCF composite ceramics are shown in Fig. 13. The prediction by MGa equation fits the experimental data well over the whole range of compositions, while those of other equations are higher than the measured data.

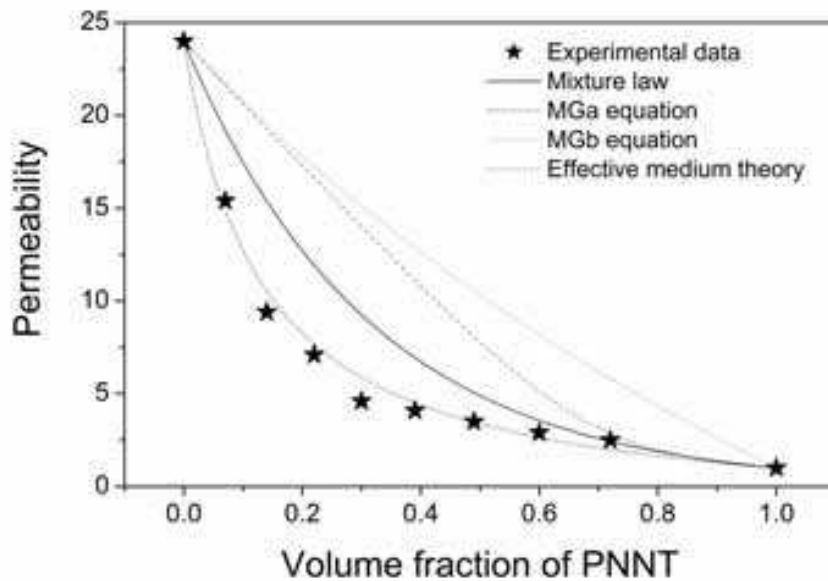


Fig. 13. The composition dependence of measured and calculated permeability of the composite ceramics of PNNT-BZCF

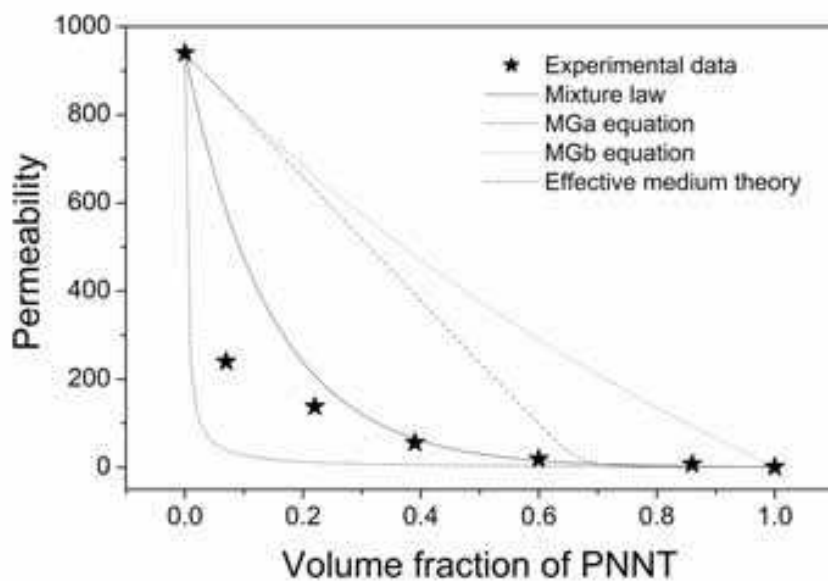


Fig. 14. The composition dependence of measured and calculated permeability of the composite ceramics of PNNT-NiCuZn ferrite

To further check the applicability of these mixture theories for permeability, the composite ceramics of PNNT-NiCuZn ferrite is discussed, where NiCuZn ferrite has a high permeability of ~ 950 (Shen et al., 2005). Fig. 14 compared the measured permeability and the values calculated by different equations. The permeability predicted by mixture law, MGa and EMT equations matches the experimental data well when the ferrite amount is relatively low. For the composite material with high volume fraction of magnetic phase, all the equations can not give precise predictions. Although an exact prediction is not presented, the MGa and MGb predictions give the upper and lower limits to the permeability of composition material.

The mixture equation based on a single simple model of microstructure may be inadequate to predict the effective macroscopic dielectric or magnetic properties over the whole composition range, so more complex equations with two or more models will be used to achieve wider applicability and more precise prediction.

5. The electromagnetic resonance character in hyper-frequency

5.1 The dielectric resonance

The frequency dispersion character is as important as the values of permittivity and permeability for the application in high frequency range. Different dispersion characters are needed by different applications. For example, capacitor or inductor requires a stable permittivity or permeability and low loss in a certain frequency range, so the resonance limits its working frequency range; while filter or EMI component needs high loss around the dielectric or magnetic resonance frequency. In a composite material, the frequency dispersion is determined by the intrinsic properties of constituent phases and affected by the interaction between them.

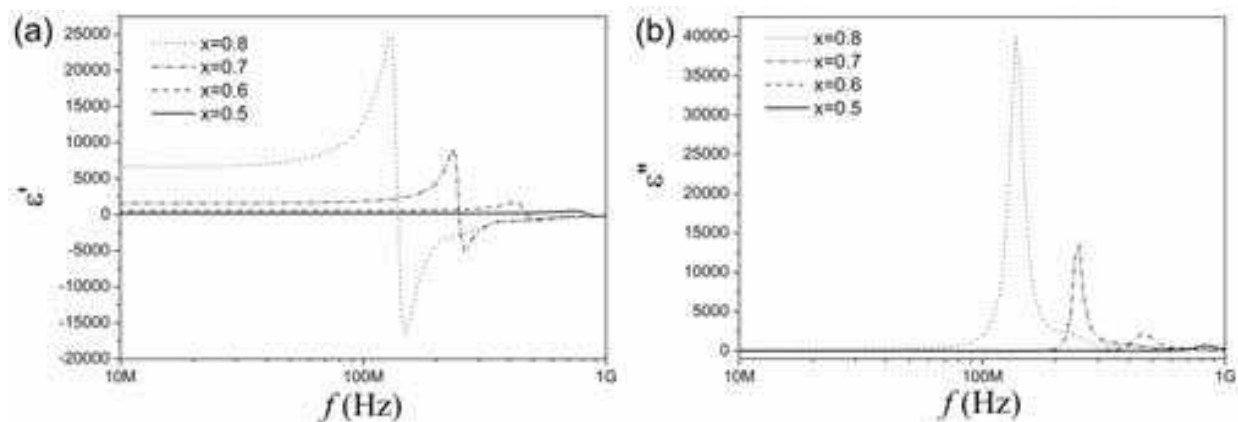


Fig. 15. Frequency dispersion of (a) real part and (b) imaginary part of permittivity of PNNT-BZCF composite ceramics

The frequency dispersion of real part and imaginary part of permittivity of PNNT-BZCF composite ceramics is shown in Fig. 15 (a) and (b). A strong dielectric resonance peak is observed above 100MHz, which originates from the dipole's vibration (Bai et al., 2006) or the followed piezoelectric vibration (Ciomaga et al., 2010). The resonance frequency increases with the reduction of PNNT amount and shifts out of the upper limit of measurement when the weight fraction of PNNT is lower than 0.4 (Fig. 16). In addition, the resonance peak turns flatter with the reduction of PNNT amount, which is characterized as the variation of half peak breadth in Fig. 17. The change of the shape of resonance peak implies that the dielectric response tends to transform from resonance to relaxation.

In addition to the intrinsic properties of constituent phases, the electromagnetic interaction between ferroelectric and ferromagnetic phases influences the frequency and shape of resonance peak. The charged particles in ferroelectric phase vibrate under the force of external electric field. When the frequency of alternating electric field matches the nature frequency of the charged particles' vibration, dielectric resonance occurs. In the ferroelectric-ferromagnetic composite material, the spatial inhomogeneous electromagnetic field around ferrite grains will disturb the charged particles' motion in ferroelectric phase and change

their nature frequency. The equivalent damping for the charged particles' motion increases with the enhancement of magnetic phase, so the dielectric response changes from resonance to relaxation gradually. Since the macroscopic frequency spectra of permittivity reflects the statistical average effect of microscale charged particles, the resonance peak turns flatter and shifts to higher frequency with the rise of ferrite amount.

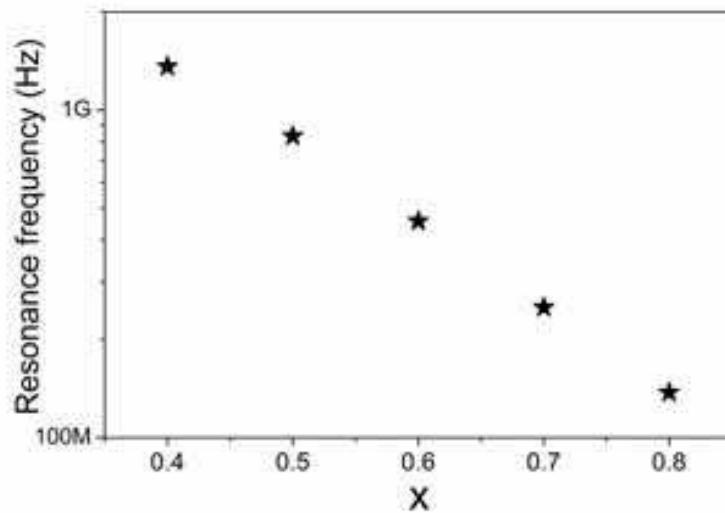


Fig. 16. The composition dependence of dielectric resonance frequency of PNNT-BZCF composite ceramics

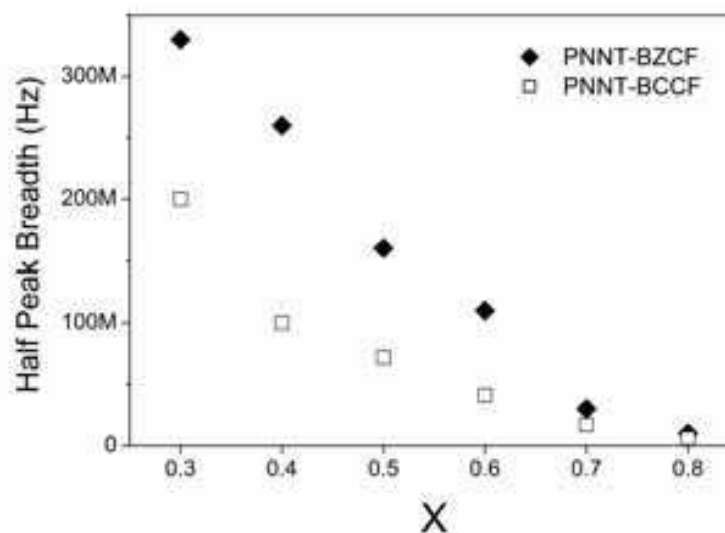


Fig. 17. The composition dependence of the half peak breadth of dielectric resonance peak for PNNT-BZCF and PNNT-BCCF composite ceramics

The electromagnetic interaction between two phases is affected by the permeability of magnetic phase. Fig. 17 (a) compares the dielectric dispersions of PNNT-BZCF and PNNT-Ba₂Co_{1.2}Cu_{0.8}Fe₁₂O₂₂ (BCCF) composite ceramics with same composition ratio, where BZCF and BCCF have identical properties in sintering character, microstructure, permittivity, and electric resistivity, except for in permeability. The permeability of BZCF (>20) is much higher than that of BCCF (~3.5). From Fig. 18, two composite materials have same dielectric

behavior of permittivity except for the distinctly different resonance characters. The dielectric resonance peak of PNNT-BCCF composite ceramics is narrow and sharp, while that of PNNT-BZCF composite ceramics is much wider and smoother. The comparison of half peak breadth shows the contrast in Fig. 17. The induced magnetic field around ferrite particles is enhanced with the permeability of ferrite, but the variation of electromagnetic environment is not strong enough to change the value of permittivity within low frequency range and can only vary the resonance character, which is sensitive to surrounding condition.

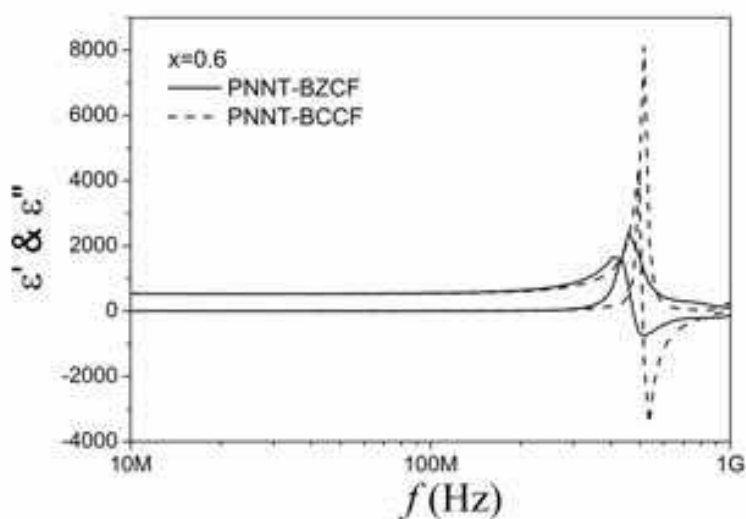


Fig. 18. The comparison of the dielectric frequency spectra of PNNT-BZCF and PNNT-BCCF composite ceramics

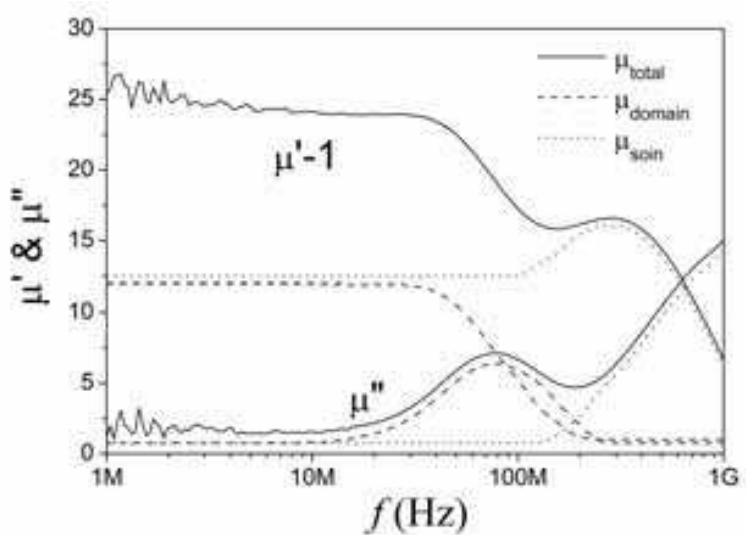


Fig. 19. Frequency spectrum of permeability of BZCF and the divided contributions of domain wall motion and spin rotation

5.2 The magnetic resonance

The frequency dispersion of permeability of ferroelectric-ferromagnetic composite ceramics is determined by the nature of magnetic phase. In the frequency spectra of a soft magnetic

ferrite, there will be some kinds of resonances, such as magnetic domain wall resonance and spin resonance. As shown in Fig. 19, there are two resonance peaks in the frequency spectra of permeability, where the low-frequency peak originates from the domain wall resonance and the high-frequency peak results from the spin resonance (Bai et al., 2004). The permeability can be divided into two parts according to the contributions of domain wall motion and spin rotation, $\mu_{\text{total}} = \mu_{\text{domain}} + \mu_{\text{spin}}$, as shown in Fig. 19.

For the composite ceramics with high ferrite fraction, there are still two resonance peaks in the frequency spectra (Fig. 19). With the reduction of BZCF amount, the permeability decreases, and the resonance peaks turn flatter and weaker gradually on account of dilution effect.

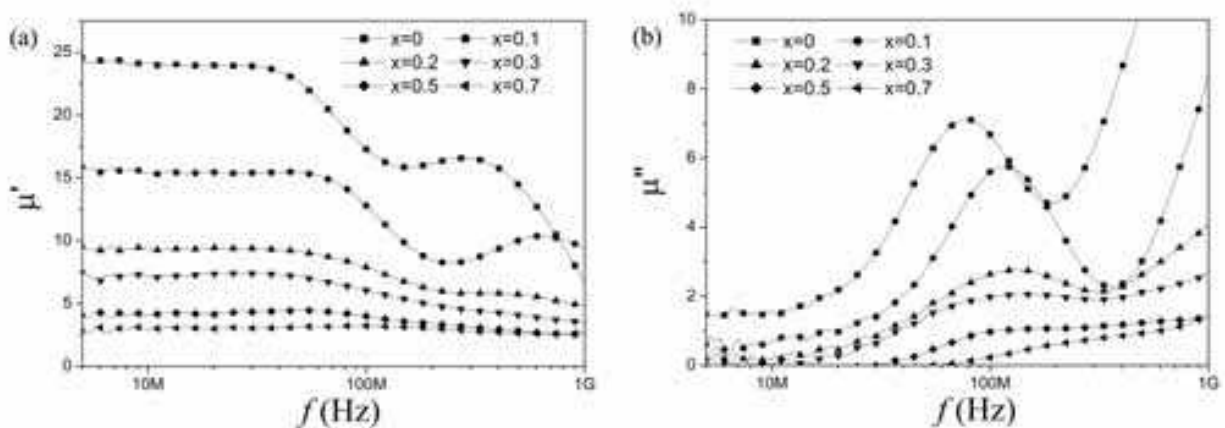


Fig. 20. Frequency dispersion of (a) real part and (b) imaginary part of complex permeability of PNNT-BZCF composite ceramics

The frequency dispersion of composite ceramics' permeability is influenced by the microstructure, such as internal stress. For the samples with large BZCF amount ($x < 0.3$), two resonance peaks appear in the frequency spectra of permeability. Spin rotation is much sensitive to the internal stress on magnetic particles, so the spin resonance peak disappears when $x > 0.2$. In contrast, the domain wall resonance peak exists up to $x = 0.7$.

6. Summary

With the rapid development of electronic products, the multi-functional ferroelectric-ferromagnetic composite materials are great desired by various novel electronic components and devices. Then various composite systems and preparation methods were widely investigated and encouraging progresses have been made. To avoid co-firing mismatch and achieve a fine microstructure, the materials with similar densification behavior are desired as the constituent phases in the composite ceramics. And low sintering temperature is needed not only by the technical requirement of LTCC but also to avoid the element diffusion, volatilization and formation of other phase.

To keep up with the trend towards higher frequency for electronic technology, the composite materials with both high permittivity and permeability in hyper frequency is developed in recent years. The co-fired composite ceramics of $0.8\text{Pb}(\text{Ni}_{1/3}\text{Nb}_{2/3})\text{O}_3$ - $0.2\text{PbTiO}_3/\text{Ba}_2\text{Zn}_{1.2}\text{Cu}_{0.8}\text{Fe}_{12}\text{O}_{22}$ are mainly introduced in this chapter, which has excellent co-firing behavior, dense microstructure and good electromagnetic properties. Owing the intrinsic characters of constituent phases, the composite ceramics exhibit both ferromagnetic

and ferroelectric properties over a wide composition range, and it has both high permittivity and high permeability in hyper-frequency, which can be tuned by the relative fraction of phases.

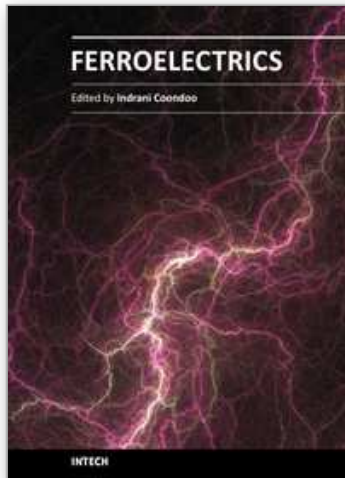
In the development of novel composite materials, the prediction of effective electromagnetic properties is greatly needed for material design. In this chapter three popular mixture theories, mixture law, Maxwell-Garnett equations and Bruggeman effective medium theory, have been introduced. In most cases, these theories can give a rough prediction for permittivity and permeability, or provides upper and lower limits, while the predictions departs from the experimental data great in some conditions. Hence, more complex equations with two or more models are being investigated.

7. References

- Aspnes, D. E. (1982). Local-field effects and effective-medium theory: A microscopic perspective, *Am. J Phys.*, vol. 50, pp.704-709
- Bai, Y.; Zhou, J.; Gui, Z. & Li, L. (2004). Frequency dispersion of complex permeability of Y-type hexagonal ferrites, *Mater. Lett.*, vol. 58, pp. 1602-1606
- Bai, Y.; Zhou, J.; Sun, Y.; Li, B.; Yue, Z.; Gui, Z. & Li, L. (2006). Effect of electromagnetic environment on the dielectric resonance in the ferroelectric-ferromagnetic composite, *Appl. Phys. Lett.*, vol. 89, pp. 112907
- Bai, Y.; Zhou, J.; Gui, Z.; Li, L & Qiao, L. (2007). A ferromagnetic ferroelectric cofired ceramic for hyper-frequency, *J Appl. Phys.*, vol. 101, pp. 083907
- Bai, Y.; Xu, F.; Qiao, L. & Zhou, J. (2009). The modulated grain morphology in co-fired composite ceramics and its influence on magnetic properties, *J Magn. Magn. Mater.*, vol. 321, pp. 148-151
- Ciomaga, C. E.; Dumitru, I.; Mitoseriu, L.; Galassi, C.; Iordan, A. R.; Airimioaic M. & Palamaruc M. N. (2010). Magnetolectric ceramic composites with double-resonant permittivity and permeability in GHz range: A route towards isotropic metamaterials, *Scripta Mater.*, vol. 62, pp. 610-612
- Bruggeman, D. A. G. (1935). Berechnung verschiedener physikalischer Konstantenvon heterogenen Substanzen, *Ann. Phys. (Leipzig)*, vol. 24, pp. 636-679
- Hill, N. A. (2000). Why are there so few magnetic ferroelectrics? *J Phys. Chem. B.*, vol. 104, pp. 6694-6709
- Hsu, R. T. & Jean, J. H. (2005). Key factors controlling camber behavior during the cofiring of bi-layer ceramic dielectric laminates, *J Am. Ceram. Soc.*, vol. 88, pp. 2429-2434
- Kanai, T.; Ohkoshi, S.; Nakajima, A.; Nakajima, A.; Watanabe, T. & Hashimoto, K. (2001). A ferroelectric ferromagnet composed of $(\text{PLZT})_x(\text{BiFeO}_3)_{1-x}$ solid solution, *Adv. Mater.*, vol. 13, pp. 487-490
- Kumar, M. M.; Srinath, S.; Kumar, G. S. & Suryanarayana, S. V. (1998). Spontaneous magnetic moment in $\text{BiFeO}_3\text{-BaTiO}_3$ solid solutions at low temperatures, *J Magn. Magn. Mater.*, vol. 188, pp. 203-212
- Maxwell Garnett, J. C., (1904). Colours in metal glasses and in metallic films, *Philos. Trans. R. Soc. London*, vol. 203, pp. 385-420
- Maxwell Garnett, J. C., (1906). Colours in metal glasses, in metallic films, and in metallic solutions. II, *Philos. Trans. R. Soc. London*, vol. 205, pp. 237-288
- Qi, X.; Zhou, J.; Yue, Z.; Li, M. & Han, X. (2008). Cofiring behavior of ferroelectric ferromagnetic composites, *Key Eng. Mater.*, vol. 368-372, pp. 573-575

- Qi, X.; Zhou, J.; Li, B.; Zhang, Y.; Yue, Z.; Gui, Z. & Li L. (2004). Preparation and spontaneous polarization-magnetization of a new ceramic ferroelectric-ferromagnetic composite, *J Am. Ceram. Soc.*, vol. 87, pp. 1848-1852
- Qi, X.; Zhou, J.; Yue, Z.; Gui, Z.; Li L. & Buddhudu S. (2004). A ferroelectric ferromagnetic composite material with significant permeability and permittivity, *Adv. Func. Mater.*, vol. 14, pp. 290-296
- Shen, J.; Bai, Y.; Zhou, J. & Li, L. (2005). Magnetic properties of a novel ceramic ferroelectric-ferromagnetic composite, *J Am. Ceram. Soc.*, vol. 88, pp. 3440-3443

IntechOpen



Ferroelectrics

Edited by Dr Indrani Coondoo

ISBN 978-953-307-439-9

Hard cover, 450 pages

Publisher InTech

Published online 14, December, 2010

Published in print edition December, 2010

Ferroelectric materials exhibit a wide spectrum of functional properties, including switchable polarization, piezoelectricity, high non-linear optical activity, pyroelectricity, and non-linear dielectric behaviour. These properties are crucial for application in electronic devices such as sensors, microactuators, infrared detectors, microwave phase filters and, non-volatile memories. This unique combination of properties of ferroelectric materials has attracted researchers and engineers for a long time. This book reviews a wide range of diverse topics related to the phenomenon of ferroelectricity (in the bulk as well as thin film form) and provides a forum for scientists, engineers, and students working in this field. The present book containing 24 chapters is a result of contributions of experts from international scientific community working in different aspects of ferroelectricity related to experimental and theoretical work aimed at the understanding of ferroelectricity and their utilization in devices. It provides an up-to-date insightful coverage to the recent advances in the synthesis, characterization, functional properties and potential device applications in specialized areas.

How to reference

In order to correctly reference this scholarly work, feel free to copy and paste the following:

Yang Bai (2010). The Ferroelectric-Ferromagnetic Composite Ceramics with High Permittivity and High Permeability in Hyper-Frequency, *Ferroelectrics*, Dr Indrani Coondoo (Ed.), ISBN: 978-953-307-439-9, InTech, Available from: <http://www.intechopen.com/books/ferroelectrics/the-ferroelectric-ferromagnetic-composite-ceramics-with-high-permittivity-and-high-permeability-in-h>

INTECH
open science | open minds

InTech Europe

University Campus STeP Ri
Slavka Krautzeka 83/A
51000 Rijeka, Croatia
Phone: +385 (51) 770 447
Fax: +385 (51) 686 166
www.intechopen.com

InTech China

Unit 405, Office Block, Hotel Equatorial Shanghai
No.65, Yan An Road (West), Shanghai, 200040, China
中国上海市延安西路65号上海国际贵都大饭店办公楼405单元
Phone: +86-21-62489820
Fax: +86-21-62489821

© 2010 The Author(s). Licensee IntechOpen. This chapter is distributed under the terms of the [Creative Commons Attribution-NonCommercial-ShareAlike-3.0 License](#), which permits use, distribution and reproduction for non-commercial purposes, provided the original is properly cited and derivative works building on this content are distributed under the same license.

IntechOpen

IntechOpen